

Image Processing of the Film Fluid Flow in a Spinning Disk Reactor

Dmitry Goldgof, Valentina Korzhova, Grigori Sisoiev

Department of Computer and Science
University of South Florida, USA
School of Mathematics
University of Birmingham, UK

goldgof@csee.usf.edu korzhova@scee.usf.edu

G.Sisoiev@bham.ac.uk

Abstract

This paper presents novel video-based algorithms for detection and tracking of spiral waves of fluid in a spinning disk reactor. One of the algorithms is based on processing of experimental video data consisting of the discrete field of disk point coordinates and its intensities. Another algorithm is based on the mathematical models of Navier-Stokes type for the thin film flow. Comparison of the results for these two algorithms is made. Ill-posed problems of estimation of characteristics of wave regimes such as a radial velocity component and inclination angles are considered. To estimate errors of the respective estimates, the so-called quasi-optimal method is implemented.

1. Introduction

The flow of a liquid film over a rapidly rotating horizontal disk has been used in many industrial applications. They range from a magnetic disk with a thin lubricant film to processes involving heat or mass transfer between expanded liquid and surrounded gas, blood oxygenation, and cooling devices.

Experimental observations [1, 2, 3, 4, 5] have demonstrated that at a small flow-rate, a smooth film is formed, and at a moderately higher flow-rate, circumferential waves moving from the disk center to the disk periphery are formed. Further increasing flow rate leads to the appearance of spiral waves unwinding in the direction of rotation [6].

Theoretical explanation of experimental results has received increasing attention in recent published research. In recent papers [9, 10, 11] an evolution system of equations to model axis-symmetric finite-amplitude waves was derived and analyzed; this model was extended for non-axis-symmetric flows to explain the experimental results. Nevertheless, the theory here is based on a general system of the Navier-Stokes equations, which are very difficult to investigate. Therefore, many problems should be treated by parallel application of theo-

retical and experimental approaches: sensitivity of wave regimes to flow conditions and the three-dimensional structures observed in experiments.

Recently, work has begun in an effort to combine precise experimental setup, theoretical derivation, and basic image analysis techniques [5]. The motion analysis of non-rigid objects and the analysis of fluid-like motion were attempted [12, 13, 14, 15]. For the fast fluid-like motion in the air, having turbulent character, detection of interface between fluid and air is important. A special so-called particle image velocimetry (PIV) technique was developed [16] to measure the kinematics of turbulent fluid flow in controlled laboratory experiments. Given a typical ensemble of PIV images, the aim is to calculate the instantaneous interface, including the instantaneous velocity on the surface of the fluid with air contact, efficiently and with a reasonable degree of accuracy. Algorithms used are typically based on a filter-like approach. In practice, however, experimental data, obtained for a sequence of time instants, contain information that, generally speaking, differs from the model variables.

Algorithms and analysis of spiral waves in a spinning disk reactor are presented in [17]. Also, the characteristics of wave regimes such as wavelength and inclination angles and their accuracy were estimated and results computed from video data were compared with results predicted by the theoretical model [11].

The purpose of this paper is to develop an automated system of detecting and tracking of the film flow over a spinning disk with intention of detecting regimes of the fluid flow, to develop the respective algorithms for that system; in particular, to calculate fluid flow parameter such as a radial velocity component and to compare them with the solution of the mathematical models. In this paper, combination of direct visualization with image analysis software, utilizing results and methods of mathematical modeling, is suggested.

2. Data Acquisition

The experimental set-up is shown in Figure 1. It consists

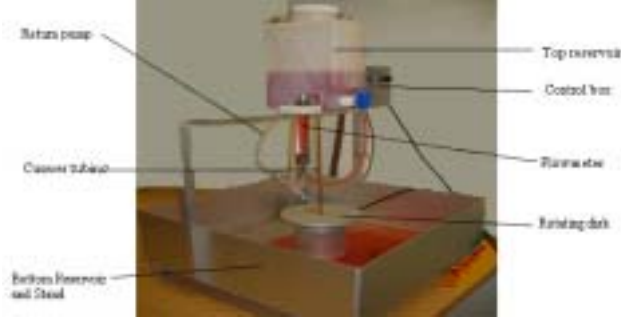


Figure 1: Experimental Setup.

of a motor; aluminum flat/round stock; reservoir; tubing; brass adapters; bunged cords; flow-meter; copper tubing; aluminum control box; switches; return pump; miscellaneous hardware. The main characteristic of motor is given by the turntable calibration.

Measurements of fluid flow were performed in controlled laboratory experiments in the same way as in [17]. Water contained in a plastic container with an adjustment valve for the flow was drained through copper tubing at a constant flow rate, which can be changed in the range 0.2-0.8 *lpm* (liter per minute). Water emerged from the nozzle pouring out onto the center of a constantly rotating aluminum disk with a rough surface. The rotational frequency of the disk was monitored by a motor control. The actual frequency can be measured with an accuracy 1/100 *rpm* (reverses per minute). Water leaving the rotating disk is collected at the bottom reservoir and picked up to the top reservoir by a pump.

The series of videos were taken at different parameter settings (different arrangements of light and settings of the camera) using the portable camcorder Canon Optura 20, capable of capturing images at 30 *fps* (frame per second). Figure 2 shows images of the liquid film that flows over a disk rotating with the angular velocity of 320 *rpm* and 520 *rpm* with the flow rate 0.8 *lpm* respectively. One of the resulted images can be seen in (Figure 2).

The technique described in [18] was used for calculating the intrinsic and extrinsic parameters of the camera.

3. Algorithms and results

3.1. Spiral detection algorithm

We consider the spiral below as periodic functions due to their stationary property [3] with respect to the rotating disk. Let $\Delta\Phi$ be the period of the spiral equations in the polar system of coordinates $r = r_j(\phi) : r_j(\phi + \Delta\Phi) = r_j(\phi)$, $\Delta\phi$ be the angle-step of the calibration in the polar

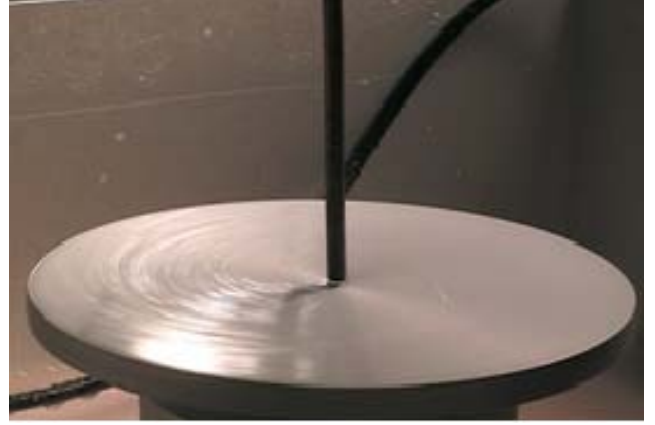


Figure 2: Rotating Disk Closeup.

system coordinates, $N = \frac{\Delta\Phi}{\Delta\phi} > 1$ is integer, and

$$\phi = \phi_i = \phi_0 + i\Delta\phi, \quad i = 1, 2, \dots, N;$$

$$r_j(\phi_0) = r_0 = \min r_j(\phi);$$

$$r_0 < r_{i1} < r_{i2} < \dots < r_{iS} \leq 200,$$

$$r_{ij} = r_j(\phi_i), \quad i = 1, 2, \dots, N, \quad j = 1, \dots, S, \quad (4)$$

where S is the number of spirals for each i , r_{ij} are experimental data for $\phi = \phi_i$; the points (ϕ_i, r_{ij}) are on the respective spirals. Then

1st spiral: $(\phi_1, r_{11}), (\phi_2, r_{21}), (\phi_3, r_{31}), \dots, (\phi_N, r_{N1});$
 $(\phi_{N+1}, r_{12}), (\phi_{N+2}, r_{22}), \dots, (\phi_{2N}, r_{N2}); \dots;$
 $(\phi_{(S-1)N+1}, r_{1S}), (\phi_{(S-1)N+2}, r_{2S}), \dots, (\phi_{SN}, r_{NS});$

2d spiral: $(\phi_{N+1}, r_{11}), (\phi_{N+2}, r_{21}), (\phi_{N+3}, r_{31}), \dots,$
 $(\phi_{2N}, r_{N1}); (\phi_{2N+1}, r_{12}), (\phi_{2N+2}, r_{22}), \dots, (\phi_{3N}, r_{N2});$
 $\dots; (\phi_{SN+1}, r_{1S}), (\phi_{SN+2}, r_{2S}), \dots, (\phi_{2SN}, r_{NS}); \dots;$

(n+1)th spiral: $(\phi_{nN+1}, r_{11}), (\phi_{nN+2}, r_{21}),$
 $(\phi_{nN+3}, r_{31}), \dots, (\phi_{(n+1)N}, r_{N1}); (\phi_{(n+1)N+1}, r_{12}),$
 $(\phi_{(n+1)N+2}, r_{22}), \dots, (\phi_{(n+2)N}, r_{N2}); \dots;$
 $(\phi_{(n+S-1)N+1}, r_{1S}), (\phi_{(n+S-1)N+2}, r_{2S}), \dots,$
 $(\phi_{(n+S)N}, r_{NS}).$

Let

$$R_{ij}, \quad i = 1, \dots, N, \quad j = 1, \dots, S,$$

be the given data on the contracted disk in the form of the standard ellipse with the parameters $a = R = 100 \text{ mm}$ and $0 < b < R$, $b \approx 35 \text{ mm}$. Then

$$r_{ij} = r_j(\phi_i) = R_{ij} \frac{R}{[(a \cos \phi_i)^2 + (b \sin \phi_i)^2]^{1/2}},$$

where $\phi_0 = 0$, and $i = 1, \dots, N$, $j = 1, \dots, S$.

Let Δr be the radius-step of calibration in the polar system coordinates, and

$$(\phi_i, k\Delta r; I_{ik}), \quad i = 1, 2, \dots; \quad k = 1, 2, \dots,$$

be the calibration net on the contracted disk, where I_{ik} are the intensities of the points $(\phi_i, k\Delta r)$. Then

$$R_{ij} = \frac{1}{2M} \sum_{k=j-M}^{j+M} k\Delta r; \quad I_{ik} \neq 0,$$

$$k = j - M, j - M + 1, \dots, j + M;$$

$$i = 1, 2, \dots, N; \quad j = 1, 2, \dots, S,$$

where $2M$ means maximal number of pixels in the vicinity of the point (ϕ_i, R_{ij}) along the radius with the angle ϕ_i and with the center in that point. The detected points on the wave of the given sector $\Delta\Phi$ is shown in Figure 3.

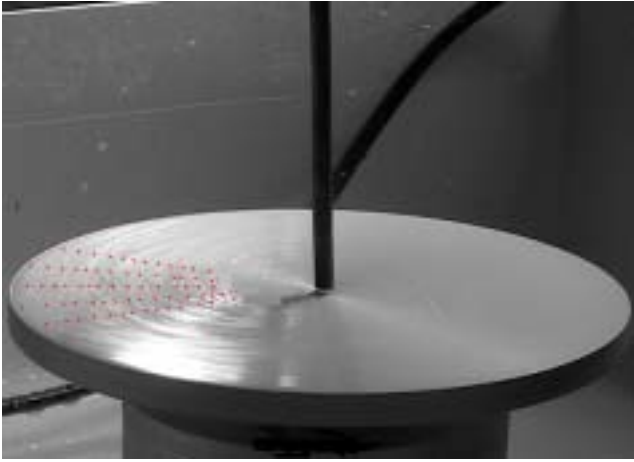


Figure 3: The detected points on the wave of the given sector of the disk.

3.2. Determination of velocity of spiral waves

To determine the velocity of wave, the sequences of the images of the film flows are used with the time difference equaled to $\Delta t = |t_2 - t_1| \text{ sec}$. Choosing the system of coordinates at the center of the rotation disc, the changes of the radii at the different times are calculated: $\Delta r = |r_2 - r_1|$, where r_1 is the value of the radius from center to the point on the wave at the moment t_1 and r_2 at the moment t_2 . The estimate of the radial velocity component $r'_{exp} = \frac{\Delta r}{\Delta t}$. To estimate Δt the azimuthal angle $\Delta\phi = \frac{2}{5} \text{ radian}$ between r_1 and r_2 is used.

The problem of determination of velocity of wave is ill-posed, i.e., for such problems, arbitrary small errors of the initial data can give, in general, arbitrary large errors of the respective results. For the proper experimental estimation of derivatives, the estimates of the maximal absolute values of the first and the second derivatives

are required. That information can be obtained due to the model of spirals of the flow waves [17]. Though that model does not regard all conditions of the film flow as the equations of Navier Stokes, it has the right relations for good estimates of the required maximal values of the first and second derivative of the motion. Using these values, the quasi-optimal $\Delta t \approx 1/100 \text{ s}$ for the quasi-optimal estimation of the first derivatives $r(t)$. Note, this value for Δt agree rather well with the quantization error of images. Then, the respective error for estimation of the velocity of wave with regarding to randomizing $\frac{\Delta}{M_1} \approx 0.065$. The radii and the averaged experimental velocity of wave for one sequence of images (with disk rotation 520 rpm and flow rate 0.8 lpm) are given in Table 1. The averaged velocity of wave over five videos

Table 1: Experimental Velocity of Wave.

Radii (cm)	Δr (cm)	Velocity of wave (cm/s)
4.0	0.804	80.4
4.5	0.77	77.4
5.0	0.748	74.8
5.5	0.704	70.4
6.0	0.684	68.4
6.5	0.660	66.0
7.0	0.636	63.6
7.5	0.612	61.2
8.0	0.594	59.4
8.5	0.564	56.4
9.0	0.552	55.2
9.5	0.534	53.4

and predicted velocity of steady flow are shown in Figure 4. The qualitative behavior of the velocity of wave, according to Table 1 and Figure 4, is quite similar to the asymptotic theory [3, 10]. However, the quantitative experimental and predicted values are different. It can be explained by the fact that the predicted values were calculated for the surface steady fluid flow.

4. Conclusion

Thus, processing of the fluid flow experimental data obtained with the help of a single camera has the respective video image of spirals of waves, confirming the asymptotic theory of the Navier-Stokes equations for the thin film. The five videos with the sequence of ten frames of each of them for the flow rate of 0.8 lpm and the rotation of disk of 520 rpm were used for determination of the velocity of wave (see Table 1). Average results of calculated velocity of wave and theoretically predicted velocity of steady flow are shown in Figure 4. The velocity of wave, as predicted, decreases as a radius increases.

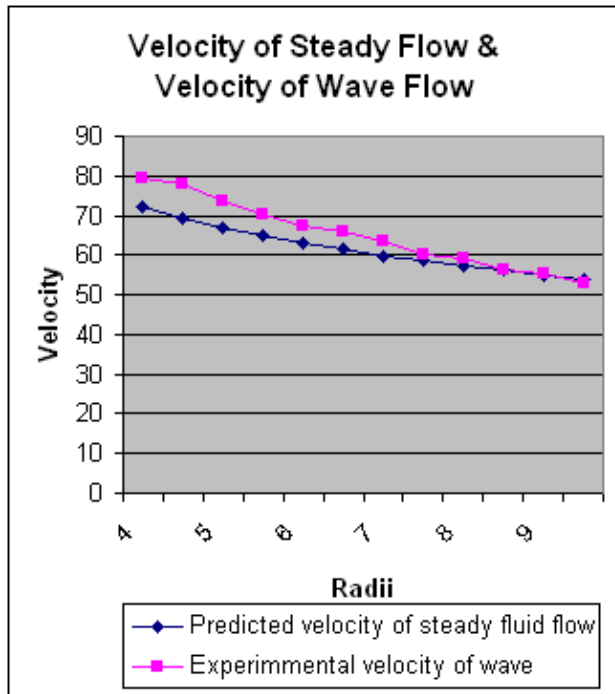


Figure 4: The relation of the averaged experimental velocity of wave and the radii (series 2); the relation of theoretical steady flow and radii (series 1).

5. References

- [1] Aoune, A. and Ramshaw, C., "Process intensification: heat and mass transfer characteristics of liquid films on rotating discs", *International Journal Heat Mass Transfer*, 42:2543–2556, 1999.
- [2] Butuzov, A. and Puhovoi, I., "On regimes of liquid film flows over a rotating surface", *Journal of Engineering Physics*, 31(2):217–224, 1976.
- [3] Lenewit, G., Roesner, K., and Koehler, R., "Surface instabilities of thin liquid film flow on a rotating disk", *Experiments in Fluids*, 26(1-2):75–85, 1999.
- [4] Rifert, V., Barabash, P., and Muzhilko, A., "Stochastic analysis of wave surface structure of liquid film flowing under centrifugal forces", *High-School Bulletin, Power Engineering*, 8:62–66, 1982.
- [5] Woods, W., "The hydrodynamics of thin liquid films flowing over a rotating disc", Ph.D. thesis, University of Newcastle upon Tyne, UK, 1995.
- [6] Lingwood, R., "An experimental study of absolute instability of the rotating-disk boundary-layer flow", *Fluid Mechanics*, 314:373–405, 1996.
- [7] Gottlieb, D., and Orszag, S., "Numerical Analysis of Spectral Methods: Theory and Applications", SIAM, 1977.
- [8] Rauscher, J., Kelly, R., and Cole, J., "An asymptotic solution for the laminar flow of thin films on a rotating disk", *Appl. Mechanics*, 40:43–47, 1973.
- [9] Matar, O., Sisoiev, G., and Lawrence, C., "Evolution scales for wave regimes in liquid film flow over a spinning disk", *Phys. Fluids*, 16:1532–1545, 2004
- [10] Sisoiev, G., Matar, O., and Lawrence, C., "Axisymmetric wave regimes in viscous liquid film flow over a spinning disk", *Fluid Mechanics*, 495:385–411, 2003.
- [11] Sisoiev, G., Matar, O., and Lawrence, C., "Stabilizing effect of the Coriolis forces on a viscous liquid film flowing over a spinning disc", *Comptes Rendus Mecanique*, 332:203–207, 2004.
- [12] Corpetti, T., Memin, E., and Perez, P., "Dense estimation of fluid flows", *IEEE Transactions on Pattern Analysis and Machine Intelligence*, 24:365–380, March 2002.
- [13] Kambhamettu, C., Goldgof, D., Terzopoulos, D., and Huang, T., "Computer Vision, Handbook of Pattern Recognition and Computer Vision", volume 2, chapter 11. Academic Press, 1994.
- [14] Zhang, J., Huang, T., and Adrian R., "Extracting 3d vortices in turbulent fluid flow", *IEEE Transactions on Pattern Analysis and Machine Intelligence*, 20:193–199, 1998.
- [15] Zhou, L., Kambhamettu, C., and Goldgof, D., P. K., and Hasler, A., "Tracking nonrigid motion and structure from 2d satellite cloud images without correspondences" *IEEE Transactions on Pattern Analysis and Machine Intelligence*, 23:1330–1336, 2001.
- [16] Misra, S., Thomas, M., Kambhamettu, C., Kirby, J., Veron, F., and Brocchini, M., "Estimation of complex air-water interfaces from particle image velocimetry images", *Experiments in Fluids*, 2006.
- [17] Goldgof, D.B., Korzhova, V.N., and Sisoiev, G.M., "Detection of Spiral Waves in Video", *ICPR 06*, 2006 (to appear).
- [18] Zhang, Z., "A flexible new technique for camera calibration", *IEEE Transactions on Pattern Analysis and Machine Intelligence*, 22:1330–1334, 2000.